Liquid Crystals

High birefringence and high resistivity isothiocyanate-based nematic liquid crystal mixtures

Sebastian Gauza[a]; Jun Li[a]; Shin-Tson Wu[a]; Anna Spadło[b]; Roman Dąbrowski[b]; Yu-Nan Tzeng[c]; Kung-Lung Cheng[c]

[a] College of Optics and Photonics, University of Central Florida, Orlando, USA [b] Institute of Chemistry, Military University of Technology, 00-908 Warsaw, Poland [c] Union Chemical Laboratory, Industrial Technology Research Institute, Hsinchu, Taiwan, ROC

PLEASE SCROLL DOWN FOR ARTICLE

High birefringence and high resistivity isothiocyanate-based nematic liquid crystal mixtures

SEBASTIAN GAUZA†, JUN LI†, SHIN-TSON WU*†, ANNA SPADŁO‡, ROMAN DĄBROWSKI‡,
YU-NAN TZENG§ and KUNG-LUNG CHENG§

†College of Optics and Photonics, University of Central Florida, Orlando, FL 32816, USA
‡Institute of Chemistry, Military University of Technology, 00-908 Warsaw, Poland
§Union Chemical Laboratory, Industrial Technology Research Institute, Hsinchu, Taiwan, ROC

The molecular structures and physical properties of several single- and double-fluorinated isothiocyanatotolane, isothiocyanatocyclohexyltolane, and isothiocyanatoterphenyl compounds are reported. Two eutectic mixtures comprising these compounds are formulated and their properties evaluated. These mixtures exhibit a high birefringence, relatively low viscosity, high resistivity, and good photo and thermal stabilities. Potential applications of these mixtures for spatial light modulators, optical phased arrays, and high speed photonics are discussed.

1. Introduction

The continuous demand on faster electro-optic response time is the driving force for developing novel nematic liquid crystal (LC) mixtures [1]. Almost all LC-related devices, such as liquid crystal display (LCD) panels, LCD TVs, spatial light modulators, and optical phased arrays (OPAs) for laser communications require faster response times. In order to achieve a fast response time, low rotational viscosity (γ_1) LC mixtures are preferred [2–4]. Another straightforward approach is to use a thin cell gap filled with a high birefringence (Δn) and low viscosity LC mixture [5, 6]. High birefringence also enhances the display brightness and contrast ratio of polymer-dispersed liquid crystal (PDLC), holographic PDLC, cholesteric LCD, and LC gels [7–10]. The most effective way to increase birefringence is to elongate the π-electron conjugation length of the LC compounds [11, 12].

Cyano (CN) and isothiocyanato (NCS) are two commonly employed polar groups for elongating the molecular conjugation. The CN group has a larger dipole moment than NCS because of its linear structure. However, due to the very strong polarization of the carbon–nitrogen triple bond, the Huckel charges of carbon and nitrogen are high and well localized [13]. Accordingly, dimers are formed by strong intermolecular interactions between the nitrile groups. This phenomenon is typically considered as the origin for a relatively high viscosity observed in cyano-based LC mixtures [14]. On the other hand, the dipole moment of the NCS group is about 30% lower than that of CN. The Huckel charges of nitrogen, carbon, and sulphur are smaller in the isothiocyanato group. The predicted intermolecular interactions by the NCS group in isothiocyanato-benzene systems are smaller than those in nitrile-based systems. Dimers are not formed and, therefore, the viscosity of such molecular systems is lower than that of nitrile-based ones [15]. Due to the longer π-electron conjugation, the NCS-based LC compounds exhibit a larger birefringence than the corresponding CN compounds. A major concern of the CN- and NCS-based LC materials is their relatively low resistivity because of ion trapping near the polyimide alignment interfaces. High resistivity leads to a high voltage holding ratio which would reduce image flickering in thin film transistor (TFT)-addressed liquid crystal displays. Recently it was reported that fluorinated NCS compounds can still maintain a high resistivity [13, 16]. So far, there has been no report on high birefringence and high resistivity mixtures based entirely on the phenyltolane, cyclohexyltolane, and terphenylisothiocyanates.

In this paper, we report some high birefringence and high resistivity isothiocyanato-tolane and-terphenyl compounds and mixtures. Two eutectic mixtures with birefringence $\Delta n \sim 0.4$ at $\lambda = 633$ nm wavelength and $T \sim 23°C$ were formulated on the basis of single- an double-laterally fluorinated NCS-tolanes.

---

*Corresponding author. Email: swu@mail.ucf.edu

The mesomorphic, physical, and electro-optic properties of the compounds and mixtures were characterized. Basic photo and thermal stabilities of these two mixtures are also discussed.

2. Experimental

Several measurement techniques were involved in characterizing the physical properties of the LC compounds and mixtures. For the electro-optic measurements, we prepared homogeneous alignment cells with cell gap $d \sim 8\,\mu m$. A linearly polarized He-Ne laser ($\lambda = 632.8$ nm) was used as the light source. The linear polarizer was placed at $45°$ with respect to the LC cell rubbing direction and the analyser was crossed. The light transmittance was measured by a photodiode detector (New Focus Model 2031) and recorded digitally by a data acquisition system (DAQ, PCI 6110) using LabVIEW. An a.c. voltage with 1 kHz square waves was used to drive the LC cell whose inner sides were coated with indium tin oxide (ITO) electrodes. On top of the ITO, the substrates were covered with a thin polyimide alignment film. Buffing induced a pretilt angle of about $2°$–$3°$. The cell was held in a Linkam LTS 350 Large Area Heating/Freezing Stage equipped with Linkam TMS94 Temperature Programmer. The phase retardation (δ) of the homogeneous cells was measured by the LabVIEW system. The LC birefringence Δn at wavelength λ and temperature T was obtained by measuring the phase retardation δ of the homogeneous cell from the following equation [11]:

$$\delta(V, T, \lambda) = \frac{2\pi d \Delta n(V, T, \lambda)}{\lambda}. \quad (1)$$

Meanwhile, the ordinary and extraordinary refractive indices of the LC samples were measured at different temperatures and different wavelengths using a multi-wavelength Abbe refractometer (ATAGO DR-M4) with circulating constant temperature bath (ATAGO 60-C3). The dielectric anisotropy ($\Delta\varepsilon$), threshold voltage (V_{th}), and elastic constants (K_{11}, K_{33}) were measured by the Automatic Property Tester (APT III) system from Displaytech. All the measurements were conducted at room temperature of $23°C$ and the applied ac voltage frequency was 1 kHz. All the thermal analyses were performed using a high sensitivity differential scanning calorimeter (DSC, TA Instrument Model Q-100). Phase transition temperatures were measured using small samples (~ 1.5 mg) at $2°C\,min^{-1}$ scanning rate. The observed LC phase transitions were confirmed by the polarizing optical microscopy (POM).

The photostability of the LC mixtures was studied under nitrogen atmosphere at room temperature. The light source (Hamamatsu LC5) was additionally fitted with visible band interference filters whose transmittance range was controlled at 430–680 nm. Molecular modelling (HyperChem molecular modelling software) was performed by running Austin Model I (AM1) and Modified Neglect of Diatomic Overlap (MNDO) calculations in order to estimate the molecular conformations, polarizability, π-electron conjugation, and total molecular length of the single LC compounds.

3. Results and discussions

3.1. *Single isothiocyanates and mixtures*

Three different groups of high birefringence LC compounds were chosen for this study. Table 1 lists the compound structures and their phase transition temperatures in relation to the different formation of the rigid core. The cyclohexyltolaneisothiocyanate (CPTP-NCS) compounds exhibit a wide nematic range, which is particularly favourable for formulating high birefringence eutectic mixtures. It is the only nematic phase observed in this group of NCS compounds. The simple tolaneisothiocyanates are desirable because their low molecular mass and linear shape contribute to minimizing viscosity while maintaining a high birefringence. However, their mesomorphic properties are not impressive [17]. Typically the two-ring 4'-alkyl-4-isothiocyanatotolanes do not exhibit a desired nematic phase, except for the pentyloxy homologue which has 3,5-laterally substituted fluoro groups at the NCS-linked phenyl ring. Replacing the alkyl chain with alkoxy increases the melting temperatures for the short chain NCS-tolanes because of the increased conjugation.

From table 1, it can be seen that the melting temperatures of the difluoro alkoxy-tolane-isothiocyanates are slightly higher than those of single fluoro-alkyl homologues. The double fluorine substitutions lower the melting temperature because of the increased molecular width. However, this effect seems weaker than the opposite effect introduced by the alkoxy group. The last group of the single compounds contains alkylterphenylisothiocyanates. Both members listed in table 1 are laterally substituted by fluorine in order to lower the melting temperature. The temperature range of the nematic phase is favourably wide. A short range smectic phase is also observed for the pentyl homologue.

Based on the phase transition temperatures and associated fusion enthalpy, we used an in-house computer program to calculate the compositions of eutectic mixtures based on the SchrÖder–van Laar

Table 1. Single compound structures, phase transition temperatures and SG-1 and SG-2 mixture compositions. All temperature listed are in °C.

Compound	R	$X1$	$X2$	Phase transition temperature	SG-1	SG-2
CPTP(3F)2NCS	2	F	H	Cr 108.5 N 239.7 I	8	9
CPTP(3F)4NCS	4	F	H	Cr 77.5 N 239.2 I	14	14

| PPP(3,5F)3NCS | 3 | F | F | Cr 107.3 N 212 I | 6 | 7 |
| PPP(3,5F)5NCS | 5 | F | F | Cr 100.0 SmA 156 N 187 I | 5 | 6 |

PTP(3F)2NCS	2	F	H	Cr 71.3 I	21	
PTP(3F)3NCS	3	F	H	Cr 76.0 I		11
PTP(3F)4NCS	4	F	H	Cr1 38.4 Cr2 40.5 (N17.4) Iso	23	
PTP(3F)5NCS	5	F	H	Cr 49.2 I	7	31
PTP(3F)7NCS	7	F	H	Cr 43.4 I		22
PTP(3,5F)O2NCS	2(O)[a]	F	F	Cr 95.4 I	5	
PTP(3,5F)O4NCS	4(O)[a]	F	F	Cr 68.3 I	6	
PTP(3,5F)O5NCS	5(O)[a]	F	F	Cr 49.5 N 56.6 I	5	

[a] The oxygen link bridge is present; R stands for an alkoxy chain in such cases.

equation [18, 19]. Detailed compositions of two examples designated as SG-1 and SG-2 are listed in table 1. Since our goal is to develop high birefringence and high resistivity LC mixtures for TFT applications, we focus on the fluorinated LC compounds. The NCS compounds are known to have high birefringence and low viscosity. However, their resistivity is not high enough for active matrix addressing. Fluorine substitution in the 3- and/or 5 position significantly enhances the resistivity of the compounds [13]. The major difference between these two mixtures is the content of the laterally difluoroalkoxy-NCS-tolanes.

Table 2 compares the electro-optic properties of SG-1 and SG-2 mixtures. These two mixtures have very

similar properties, especially their birefringences, which are nearly identical: $\Delta n = 0.38$ and 0.42 at $\lambda = 632.8$ and 532 nm respectively. We also measured their ordinary and extraordinary refractive indices at $\lambda = 450, 486, 546, 633$ and 656 nm in the temperature range 15–50°C by an Abbe refractometer. Due to the high birefringence of SG-1, some n_e values exceed the measurement range of the Abbe refractometer. Therefore, some n_e data were calculated using extended Cauchy equations [20, 21] at some wavelengths and the four-parameter model [22] at some temperatures. Furthermore, we extrapolated the experimental data measured in the visible spectral region to $\lambda = 1.55 \mu m$. This method has been proven to be reasonably accurate [22]. The extrapolated (n_e, n_o)

Table 2. Physical and electro-optic properties of SG-1 and SG-2 mixtures.

Mixture	Vth v_{rms}	ε_{II}	$\varepsilon_{\perp}$	$\Delta\varepsilon$	K_{11} pN	K_{33} pN	K_{33}/K_{11}	Δn 633/532 nm	γ_1/K_{11} ms μm^{-2}	FoM μm^2 s^{-1}	Tc °C
SG-1	1.35	21.2	4.6	16.6	15.8	29.8	1.89	0.38/0.42	12	12.0	100
SG-2	1.60	19.8	4.2	15.6	20.7	31.8	1.54	0.38/0.42	10	14.4	110

values at $\lambda = 1.55\,\mu m$ are (1.8736, 1.5144), (1.8596, 1.5103) and (1.8196, 1.5244) for SG-1 at 20, 30, and 50°C, respectively.

Figure 1 (*a*) shows the wavelength-dependent refractive indices n_e and n_o of SG-1 at $T = 20$, 30 and 50°C. Solid lines are fitting curves using the following extended Cauchy equations [20, 21]:

$$n_e = A_e + \frac{B_e}{\lambda^2} + \frac{C_e}{\lambda^4} \qquad (2a)$$

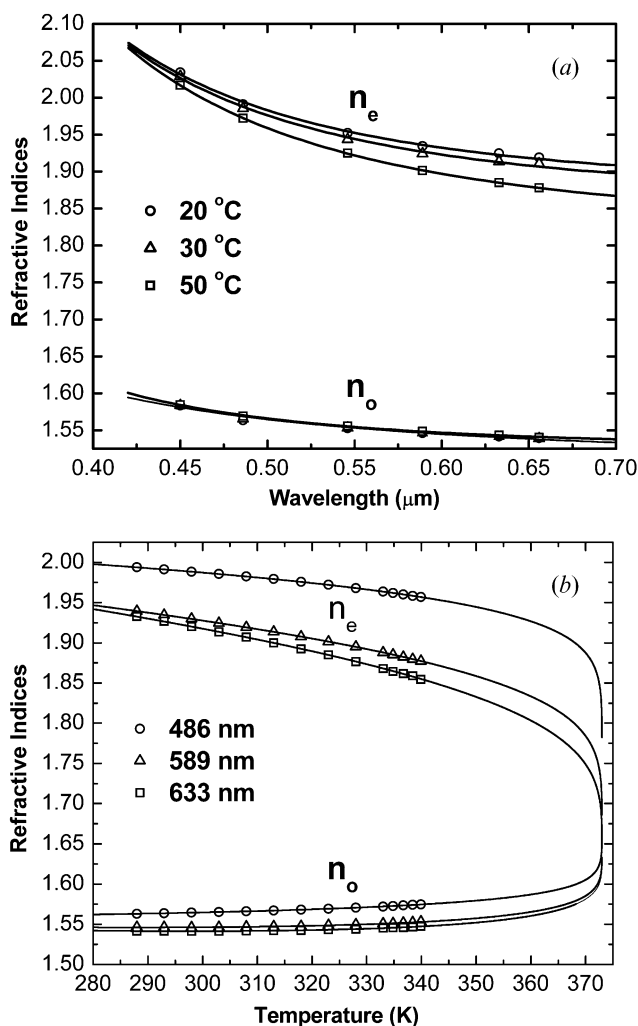$$n_o = A_o + \frac{B_o}{\lambda^2} + \frac{C_o}{\lambda^4}. \qquad (2b)$$

As the wavelength increases, both n_e and n_o decrease and then gradually saturate in the near IR region. Figure 1 (*b*) shows the temperature-dependent refractive indices of SG-1 at $\lambda = 486$, 589, and 633 nm. Solid lines are fitting curves using the following four-parameter model [22]:

$$n_e(T) = A - BT + \frac{2(\Delta n)_o}{3}\left(1 - \frac{T}{T_c}\right)^\beta \qquad (3a)$$

$$n_o(T) = A - BT - \frac{(\Delta n)_o}{3}\left(1 - \frac{T}{T_c}\right)^\beta. \qquad (3b)$$

In equation (3) $(\Delta n)_o$ is the LC birefringence in the crystalline state (or $T = 0$ K), the exponent β is a material constant and T_c is the clearing temperature of the LC material under investigation. These two parameters can be obtained by fitting the temperature-dependent Δn data. The other two parameters A and B are obtained from fitting the temperature dependent $<n(T)>$ data at a given wavelength.

From table 2, SG-1 has ~20% higher viscoelastic coefficient (γ_1/K_{11}) than SG-2. This is because SG-1 consists of a higher composition of alkoxy difluoro compounds than SG-2. The difluoro compounds exhibit a higher viscosity than the corresponding single fluoro compounds because of the increased moment of inertia. Moreover, the alkoxy group imparts a higher viscosity than the corresponding alkyl compound. For phase-only modulation using a homogeneous cell, we need to consider both phase change and response time simultaneously. A figure-of-merit (*FoM*) has been introduced to compare the performance of various LC materials [11]:

$$FoM = \frac{K_{11}(\Delta n)^2}{\gamma_1}. \qquad (4)$$

Our mixtures show impressively high *FoM* at room temperature. The *FoM* of SG-1 and SG-2 is 12.0 and 14.4 $\mu m^2\,ms^{-1}$, respectively. Under the same circumstance, the *FoM* of Merck TL-216 and E7 is ~2.4 and ~2.3 $\mu m^2\,ms^{-1}$, respectively [23]. The birefringence of Merck TL-216 and E7 was measured to be 0.20 at $\lambda = 633$ nm and $T = 22$°C. Thus, our SG mixtures show ~6X higher *FoM* than some popular commercial high birefringence LC mixtures.

3.2. Chemical and ionic purity

The chemical and ionic purity is an important concern for TFT-LCD applications because it affects the voltage

Figure 1. (*a*) Wavelength-dependent ordinary and extra-ordinary refractive indices of SG-1. Circles, triangles, and squares represent the refractive indices measured at $T = 20$, 30 and 50°C, respectively. (*b*) Temperature-dependent ordinary and extraordinary refractive indices of SG-1. Circles, triangles, and squares are measured refractive indices at $\lambda = 486$, 589, and 633 nm, respectively.

holding ratio. For an active matrix LCD, if the LC has a low resistivity then the image cannot be held steadily, i.e. images will flicker. High chemical and ion purity also elongates the lifetime of the LC devices. Long term chemical stability can be greatly improved by eliminating organic side-products during synthesis, different homologues, as well as inorganic agents involved in the processing. The compounds used in our experiment were synthesized according to state-of-the-art procedures with final chemical purity in the range 99.5–99.9 wt% [17]. In addition to their use in TFT LCDs, high resistivity LC mixtures are preferred for other electro-optic devices such as spatial light modulators and optical phased arrays based on the active driving method. Liquid crystals with a large dielectric anisotropy and high polarizability (high birefringence) tend to be more conductive [24]. To obtain high resistivity ($>10^{13}\,\Omega\,cm$) for high Δn and large $\Delta\varepsilon$ LC materials is particularly difficult.

We purified both the high birefringence mixtures using ion exchange resins in multiple-step processes. Before purification the batch size of both SG-1 and SG-2 was 25g. After only three steps of ion purification, the resistivity of SG-2 (mainly single fluorinated compounds) was improved to $10^{13}\,\Omega\,cm$ which is double that of SG-1 (mostly double-fluorinated compounds). The purification yield of SG-2 was ~65%, as estimated from the data listed in table 3. Intuitively, we would expect that the difluoro compounds should exhibit a higher resistivity than the monofluorinated compounds. Our data indicate that the monofluorinated NCS compounds are as good as the difluorinated compounds. The single-fluorinated compounds would exhibit a higher birefringence and lower viscosity, i.e. higher *FoM* than the corresponding difluoro compounds. A clear advantage of the difluoro compounds is their larger $\Delta\varepsilon$ which would lower the operating voltage.

We used molecular modelling HyperChem software to calculate the molecular dimensions, surface charges, and polarizability of the single compounds involved in our experiment. The computed molecular polarizability

can be used to find the total tensor of the polarizability. In our molecular system, we assume that the principal molecular axis is along the *x*-axis and the two much shorter molecular axes are in the orthogonal directions [25]. Under such circumstances, the polarizability tensor with respect to the principal molecular axes has a diagonal form:

$$\alpha = \begin{pmatrix} \alpha_{xx} & 0 & 0 \\ 0 & \alpha_{yy} & 0 \\ 0 & 0 & \alpha_{zz} \end{pmatrix}. \qquad (5)$$

The polarizability is dependent on the molecular structure and shape. The laterally substituted atoms would pull out the π-electrons from the main core of the molecule so that the values of α_{yy} and α_{zz} become larger. The polarizability anisotropy, i.e. the difference between, α_{xx} and α_{yy} or α_{zz}, becomes smaller.

The classical Lorentz–Lorenz equation [26] correlates the refractive index of an isotropic medium with molecular polarizability in the optical frequencies. Vuks made a bold assumption that the internal field in a liquid crystal is the same in all directions and gave a semi-empirical equation correlating the refractive indices with the molecular polarizabilities for anisotropic media [27]:

$$\frac{n_{e,o}^2 - 1}{\langle n^2 \rangle + 2} = \frac{4\pi}{3} N\alpha_{e,o} \qquad (6)$$

where n_e and n_o are refractive indices of the extraordinary ray and ordinary ray, respectively, N is the number of molecules per unit volume, $\alpha_{e,o}$ is the molecular polarizability, $\alpha_e = \alpha_{xx}$ and $\langle n^2 \rangle$ is defined as:
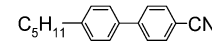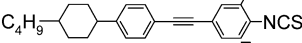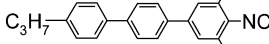
$$\langle n^2 \rangle = \left(n_e^2 + 2n_o^2 \right)/3. \qquad (7)$$

The average values of the polarizability α for our compounds are calculated and results are listed in table 4. For a uniaxial LC, the average polarizability components can be expressed in terms of the order parameter for the long molecular axis $S_{xx} = S$, and the difference between the order parameters for the short

Table 3. Resistivity (in $\Omega\,cm$) of SG-1 and SG-2 measured at the first 3–4 steps of the ion purification process; water content is in ppm.

SG-1	Resistivity	Recovery g	Water content	SG-2	Resistivity	Recovery g	Water content
Before	1.4×10^{10}	22.0	107	Before	8.2×10^{10}	23.0	96
Step 1	1.6×10^{11}	20.1	—	Step 1	7.8×10^{12}	21.3	—
Step 2	2.0×10^{12}	17.7	—	Step 2	9.5×10^{12}	18.9	—
Step 3	4.7×10^{12}	15.0	—	Step 3	1.1×10^{13}	15.0	85
Step 4	5.5×10^{12}	11.6	99				

Table 4. The calculated polarizability tensor, π-electron conjugation length (L_e), and total length (L_t) of some of the single compounds used in the SG-1 and SG-2 mixtures.

Structure	π-electron conjugation length - L_e Å	Total length - L_t Å	Polarizability (a.u.)			
			XX	YY	ZZ	α
C$_5$H$_{11}$—◯—◯—CN	9.7	15.6	270	117	112	167
C$_4$H$_9$—◯—◯—≡—◯—NCS (F)	15.0	20.7	547	189	102	279
C$_3$H$_7$—◯—◯—◯—NCS (F, F)	16.9	19.1	476	149	141	255
C$_3$H$_7$—◯—≡—◯—NCS (F)	14.9	17.3	492	180	96	239

molecular axes (S_{yy}, S_{zz}) as $D = S_{yy} - S_{zz}$. Hence,

$$\langle \alpha_{\parallel} \rangle = \alpha + \frac{2}{3} \left\{ S \left[\alpha_{xx} - \frac{(\alpha_{yy} + \alpha_{zz})}{2} \right] + \frac{D(\alpha_{yy} - \alpha_{zz})}{2} \right\} \quad (8)$$

$$\langle \alpha_{\perp} \rangle = \alpha - \frac{1}{3} \left\{ S \left[\alpha_{xx} - \frac{(\alpha_{yy} + \alpha_{zz})}{2} \right] + \frac{D(\alpha_{yy} - \alpha_{zz})}{2} \right\}. \quad (9)$$

The subscripts $\parallel$ and $\perp$ in equations (8) and (9) refer to the parallel and perpendicular directions to the director [28]. The polarizability anisotropy of our compounds is larger than that of 5CB. This is due to the elongated structures by combining the tolane unit with the highly polar isothiocyanato terminal group. An example of a single fluoro CPTP-NCS compound is shown in figure 2. The strong dipole of the carbon–fluorine bond affects the static charges distribution over the terminal part of the molecule. Particularly important is the negative charge delocalization which occurs for laterally (fluoro) substituted molecules as shown in figure 3. Molecular systems with localized strong dipoles typically tend to form dimers and attract ions. Both phenomena are undesirable, as in case of the cyano terminal group.

Inductively coupled plasma mass spectrometry (ICP-MS) was used to determine which kind of ions our SG mixtures contain. The most undesired ions found in our mixtures were aluminum, calcium and sodium positive ions. The total number of ions was measured to be below 10 ppm for both SG mixtures.

3.3. *Photo and thermal stabilities*

In many electro-optic applications using liquid crystal devices, light absorption by liquid crystal could be a critical issue in terms of material stability. The major absorption of liquid crystal compounds occurs in ultraviolet (UV) and infrared (IR) regions. In the visible

region, the absorption is usually small and can be neglected. The photostability and lifetime of a liquid crystal device are mainly affected by the electronic absorption in the UV region. According to the
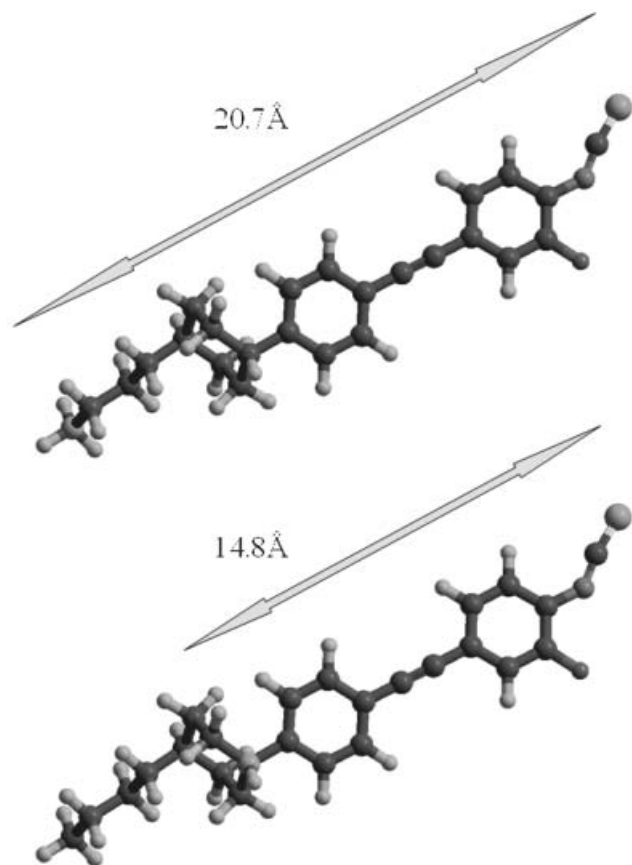

Figure 2. Molecular dimension and π-electron conjugation length of the optimized CPTP(3F)4NCS. Semi-empirical method AM1 was used for simulations.
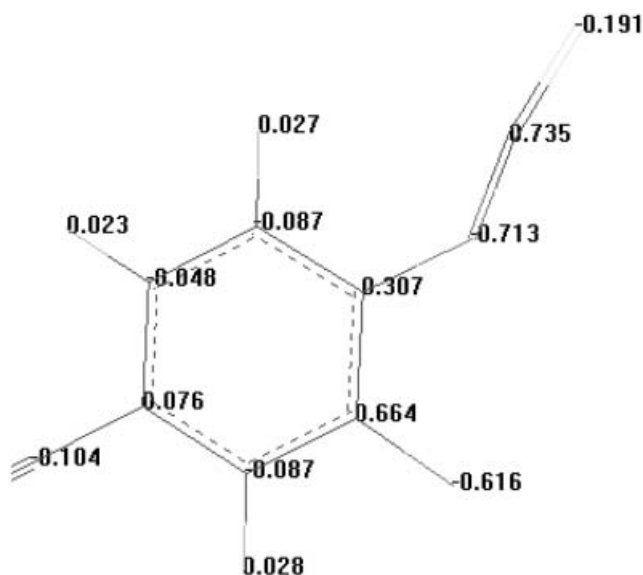
Figure 3. Huckel charge distribution calculated for an iso-thiocyanatotolane compound. Semiempirical extended Huckel method was used for calculations. Only the highly polar part of the molecule is shown.

three-band model [29], one $\sigma \rightarrow \sigma^*$ transition (designated as the λ_0 band) and two $\pi \rightarrow \pi^*$ transitions (designated as the λ_1 and λ_2 bands with $\lambda_2 > \lambda_1$) are considered. The λ_0 band is located in the vacuum UV region (λ_0 band $\sim$120 nm), and λ_1 is located between 190 and 210 nm and is in sensitive to the LC structure. The λ_2 increases substantially as the molecular conjugation increases. The high birefringence of liquid crystals originates from the elongated molecular conjugation. That is to say, the absorption peaks of high birefringence liquid crystal compounds could extend to 350–400 nm. In such a case the high energy UV photon may cause structural damage to the chemical structure of the molecules. In the IR region the absorption comes from molecular vibration bands and should not affect the LC photo-stability.

Previously, we have studied the UV absorption and stability of some tolane and terphenylisothiocyanates [30]. The UV absorption tail exceeds 365 nm—the central wavelength of a very strong emission line from the mercury or arc lamp. At this wavelength, most high birefringence liquid crystals could not survive too long an exposure. However, in most applications, we could add filters to cut off the light below 420 nm for the purpose of improving photostability and above 720 nm to avoid thermal effects. The light intensity used in the photostability studies was calibrated at λ=365 nm to be I=200 mW cm^{-2}. According to the manufacturer speci-fication, this corresponds to $I \sim$180 mW cm^{-2} at

λ=440 nm and 120 mW cm^{-2} at 550 nm which are two other strong emission lines for the mercury lamp.

Mixture SG-1 was chosen for the photostability study. The clearing temperature, optical and dielectric anisotropy, threshold voltage, and elastic constants (K_{11} and K_{33}) were measured to determine the stability of the tested mixture. However, we did not measure the resistivity because its value depends critically on the cell filling environment. The sample was exposed to 430–680 nm visible light continuously for 60 h. To avoid uneven exposure, the LC sample was stirred by a magnetic bar continuously in a nitrogen chamber. In previous experiments we learned that any damage of the molecular structure would alter the electro-optic per-formance of the mixture and decrease the clearing temperature due to composition changes [30, 31]. During the 60 h exposure, we periodically measured the electro-optic properties of the sample by filling the mixture into a homogeneous cell. Detailed results are shown in figures 4 (a–d). No degradation in birefrin-gence, dielectric constants, threshold voltage or elastic constants was observed. Thus the SG-1 mixture exhibits a reasonably good photostability, as long as the UV content of the lamp is filtered out.

Figure 5 plots the measured clearing temperature of SG-1 at different stages of exposure. The clearing temperature was measured by a DSC (TA-100). For each measurement, the same amount of illuminated sample was used. The measured clearing point remained unchanged within the course of the experi-ment.

Thermal stability is another important issue for long term operation of isothiocyanate LCs. In actual device fabrication processes, the LC mixture is usually filled into display panels in the isotropic phase and cooled to room temperature slowly in order to avoid flow marks. For laser beam steering, the LC optical phased arrays is operated at an elevated temperature ($\sim$50–70°C) in order to shorten the response time. For projection displays, the LC panel is operated at $\sim$60°C because of the thermal effect from the lamp. Therefore, it is necessary to check the thermal stability of the LC mixture at a temperature slightly above the clearing point to ensure that multiple reheating will not cause performance degradation.

We have studied the thermal stability of our high birefringence LC mixtures; in figure 6, results from of SG-2 mixture are shown. We first measured the voltage-dependent transmittance of an 8 μm homogeneous cell at room temperature. The sample cell was then kept at 125°C, which is 15° above the clearing point, for 24 h. We then repeated the same measurement at room temperature. In figure 6, the results of these two

Figure 4. Measured material stabilities of SG-1 mixture: (*a*) birefringence, (*b*) dielectric constants, (*c*) threshold voltage, (*d*) elastic constants. Light intensity: $I{\sim}180\,mW\,cm^{-2}$ at $\lambda{=}440\,nm$ and $120\,mW\,cm^{-2}$ at $\lambda{=}550\,nm$. A bulk sample was tested under nitrogen.
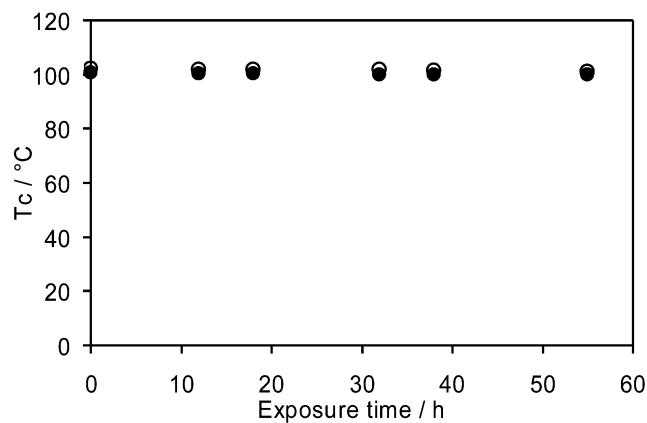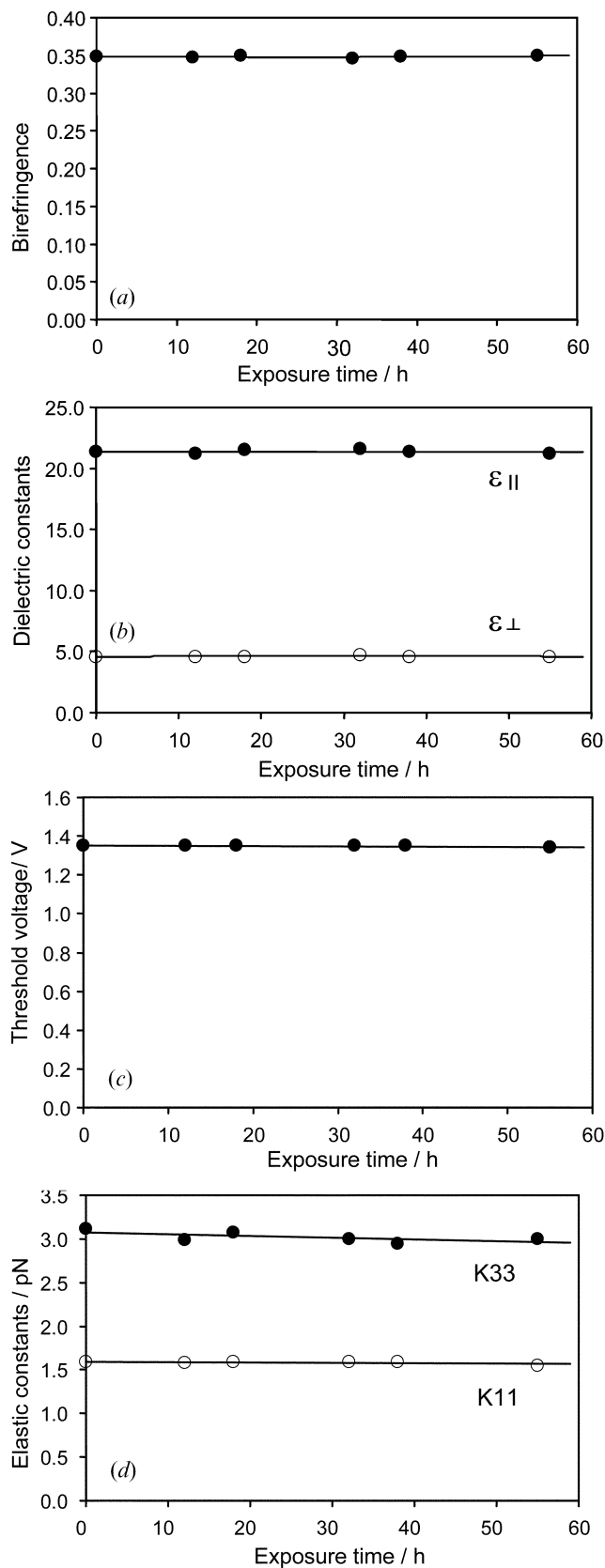

Figure 5. Clearing temperature stability measured during the photostability test of mixture SG-1. Experimental conditions are the same as those listed for figure 4. Solid and open circles are data for heating and cooling cycle of the measurements, respectively.
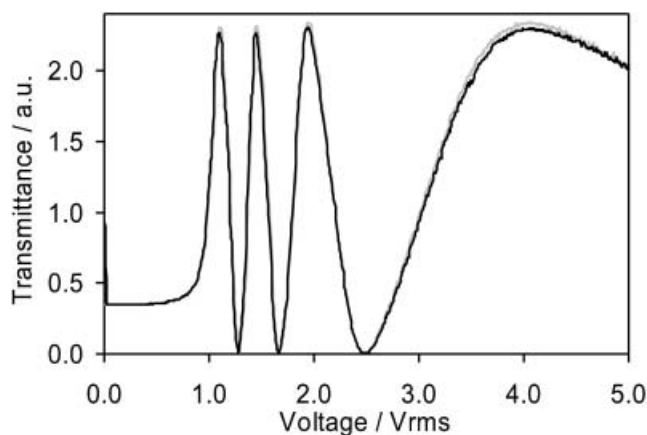

Figure 6. Voltage-dependent transmittance curves of mixture SG-1 before and after the thermal stability test. The transmittance was measured using a homogeneous cell between two crossed polarizers at $\lambda{=}633\,nm$. Grey and black solid lines represent data before and after heat exposure, respectively. Test and measurement temperature were 125°C and 25°C, respectively. The alignment layer was buffed polyimide film.

measurements overlap quite well, indicating that SG-2 exhibits a satisfactory thermal stability.

4. Conclusion

We have developed several high birefringence single- and double-fluorinated isothiocyanato tolane and

terphenyl compounds and formulated two eutectic mixtures, SG-1 and SG-2. Each mixture shows a wide nematic range, high figure-of-merit, high resistivity, and relatively good photo and thermal stabilities. Useful applications for laser beam steering, spatial light modulators, and high speed photonic devices are foreseeable.

Acknowledgment

References

[1] S.T. Wu, D.K. Yang. *Reflective Liquid Crystal Displays*, Wiley, New York (2001).

[2] S. Kibe, N. Hattori, M. Ushioda, H. Yamamoto, S. Matsui. *J. SID*, **11**, 449 (2003).

[3] T. Geelhaar, K. Tarumi, H. Hirschmann. *Soc. Inf. Display Tech. Dig.*, **27**, 167 (1996).

[4] Y. Goto, T. Ogawa, S. Sawada, S. Sugimori. *Mol. Cryst. liq. Cryst.*, **209**, 1 (1991).

[5] P.F. McManamon, T.A. Dorschner, D.L. Corkum, L. Friedman, D.S. Hobbs, M. Holz, S. Liberman, H.Q. Nguyen, D.P. Resler, R.C. Sharp, E.A. Watson. *Proc. IEEE*, **84**, 268 (1996).

[6] Y. Lu, F. Du, Y.H. Lin, S.T. Wu. *Opt. Express*, **12**, 1221 (2004).

[7] J.L. Fergason. *Soc. Inf. Display Tech. Dig.*, **16**, 68 (1985).

[8] R.L. Sutherland, V.P. Tondiglia, L.V. Natarajan. *Appl. Phys. Lett.*, **64**, 1074 (1994).

[9] N. Mizoshita, K. Hanabusa, T. Kato. *Adv. funct. Mater.*, **13**, 313 (2003).

[10] Y.H. Fan, H.W. Ren, S.T. Wu. *Appl. Phys. Lett.*, **82**, 2945 (2003).

[11] I.C. Khoo, S.T. Wu. *Optics and Nonlinear Optics of Liquid Crystals*, World Scientific, Singapore (1993).

[12] S. Gauza, C.H. Wen, S.T. Wu, N. Janarthanan, C.S. Hsu. *Jpn. J. appl. Phys.*, **43**, 7634 (2004).

[13] I.K. Huh, Y.B. Kim. *Jpn. J. appl. Phys.*, **41**, 6466 (2002).

[14] J.A. Małecki, J. Nowak. *J. mol. Liq.*, **81**, 245 (1999).

[15] J. Jadżyn, L. Hellemans, G. Czechowski, C. Legrand, R. Douali. *Liq. Cryst.*, **27**, 613 (2000).

[16] I.K. Huh, Y.B. Kim. *Jpn. J. appl. Phys.*, **41**, 6484 (2002).

[17] A. Spadło, R. Dąbrowski, M. Filipowicz, Z. Stolarz, J. Przedmojski, S. Gauza, Y.H. Fan, S.T. Wu. *Liq. Cryst.*, **30**, 191 (2003).

[18] L. Schröder. *Z. phys. Chem.*, **11**, 449 (1893).

[19] J.J. van Laar. *Z. phys. Chem.*, **63**, 216 (1908).

[20] J. Li, S.T. Wu. *J. appl. Phys.*, **95**, 896 (2004).

[21] J. Li, S.T. Wu. *J. appl. Phys.*, **96**, 170 (2004).

[22] J. Li, S. Gauza, S.T. Wu. *J. Appl. Phys.*, **96**, 19 (2004).

[23] S. Gauza, H. Wang, C.H. Wen, S.T. Wu, A.J. Seed, R. Dąbrowski. *Jpn. J. appl. Phys.*, **42**, 3463 (2003).

[24] D. Demus, Y. Goto, S. Sawada, E. Nakagawa, H. Saito, R. Tarao. *Mol. Cryst. liq. Cryst.*, **260**, 1 (1995).

[25] S.J. Clark, G.J. Ackland, J. Crain. *Europhys. Lett.*, **44**, 578 (1998).

[26] M. Born, E. Wolf. *Principles of Optics*, Pergamon Press, New York (1980).

[27] M.F. Vuks. *Opt. Spektrosk.*, **20**, 644 (1966).

[28] D.A. Dunmur, A. Fukuda, G.R. Luckhurst. *Physical Properties of Liquid Crystals: Nematics*, INSPEC, London (2001).

[29] S.T. Wu. *Phys. Rev. A*, **30**, 1270 (1986).

[30] S. Gauza, C.H. Wen, B.J. Tan, S.T. Wu. *Jpn. J. appl. Phys.*, **43**, 7176 (2004).

[31] C.H. Wen, S. Gauza, S.T. Wu. *Liq. Cryst.*, **31**, 1479 (2004).